PROCEEDINGS OF SCIENCE

Large-scale cosmic-ray anisotropies measured by the Pierre Auger Observatory

E. Roulet[a,*] **for the Pierre Auger collaboration**[b]

[a] *Centro Atómico Bariloche, Comisión Nacional de Energía Atómica*
Consejo Nacional de Investigaciones Científicas y Técnicas (CONICET)
Av. Bustillo 9500, R8402AGP, Bariloche, Argentina

[b] *Observatorio Pierre Auger, Av. San Martín Norte 304, 5613 Malargüe, Argentina*
Full author list: https://www.auger.org/archive/authors_2024_11.html

E-mail: spokespersons@auger.org

An update of the measurements of large-scale anisotropies in the arrival directions of ultra high-energy cosmic rays detected at the Pierre Auger Observatory is presented. The established dipolar anisotropy in right ascension has now reached a significance of 6.8σ when considering all energies above 8 EeV and $5.7\,\sigma$ when only considering energies between 8 and 16 EeV. The 3D dipole amplitude and direction are reconstructed in four different energy bins above 4 EeV. At energies above 8 EeV it points more than 100° away from the Galactic centre, providing evidence that the anisotropy observed is of extragalactic origin. An analysis allowing for both dipolar and quadrupolar anisotropies finds qualitatively similar dipole components and no significant quadrupole components. The results for the angular power spectrum are shown, demonstrating that no other statistically significant multipoles are present. The equatorial dipole components are presented down to 0.03 EeV using a trigger which has been optimized for low energies. We find no significant departures from isotropic expectations below 8 EeV, although below 2 EeV the phases appear to be consistently aligned with the right ascension of the Galactic centre. Finally, model predictions based on source emission scenarios obtained in the combined fit of spectrum and composition data above 0.6 EeV are discussed and compared with observations.

7th International Symposium on Ultra High Energy Cosmic Rays (UHECR2024)
17-21 November 2024
Malargüe, Mendoza, Argentina

PoS(UHECR2024)008

*Speaker

© Copyright owned by the author(s) under the terms of the Creative Commons Attribution-NonCommercial-NoDerivatives 4.0 International License (CC BY-NC-ND 4.0).
All rights for text and data mining, AI training, and similar technologies for commercial purposes, are reserved.
ISSN 1824-8039. Published by SISSA Medialab.

After two decades of operation, the Pierre Auger Observatory is entering a new phase with upgraded detectors and electronics. This marks an appropriate time to summarize and put into perspective the results obtained during Phase I of the Observatory. Here, we present the different studies related to the anisotropies on large angular scales that were performed with the measured arrival directions and discuss their possible interpretations. The establishment of a significant dipolar anisotropy for energies above 8 EeV was one of the major milestones obtained with the Auger Observatory [1, 2], together with the precise measurement of the cosmic ray (CR) spectrum that led to the observation of a strong suppression of the flux above 50 EeV [3] as well as the measurements that showed that at energies above few EeV the CR composition becomes progressively heavier [4, 5]. These and other crucial results have produced a major change in our understanding of the ultra-high energy cosmic rays (UHECRs), which are the highest energy particles that have been observed in the universe and whose origin is still uncertain.

Large angular scale anisotropies may result from the non-uniformity in the distribution of the cosmic-ray sources, from the diffusive propagation from individual sources or, at the lower energies, from the diffusive escape of the Galactic cosmic rays. Due to the expected deflections of the CRs in Galactic and extragalactic magnetic fields, combined with the observation that the composition becomes heavier as the energies increase, it is only at the highest energies that more localized anisotropies on intermediate angular scales could be expected to show up, and indeed some hints already exist suggesting their presence. In this contribution, we describe the results on large angular scale anisotropies presented in ref. [6], in which data collected over 19 years were analyzed. These include events with energies above 4 EeV with zenith angles up to 80° (covering about 85% of the sky, with a total exposure of 123,000 km^2 sr yr for the period Jan04-Dec22), as well as lower energy data down to 0.03 EeV, using both events from the surface detector array with detector spacing of 1500 m (SD-1500) having zenith angles $\theta < 60°$, as well as those with $\theta < 55°$ from the denser but smaller array with separations among detectors of 750 m (SD-750), the latter having an exposure of 269 km^2 sr yr (for Jan14-Dec21).

Several possible sources of systematic effects were accounted for, such as those due to atmospheric effects [7] or to the geomagnetic effects [8], that impact on the air-shower development and hence on the reconstruction of the CR energies. We also accounted for effects due to the non-uniformity of the exposure resulting from dead times and those related to the tilt of the array. We then checked that the final amplitudes at the solar and anti-sidereal frequencies were consistent with the absence of significant spurious effects. In the main part of the study we obtained the dipolar (and eventually also quadrupolar) amplitudes from a generalized Fourier analysis. At the lowest energies for which the detector is not fully efficient, some of the systematic effects cannot be properly evaluated, therefore we obtained just the equatorial dipole component using the East-West method [9]. This last method exploits the fact that all systematic effects are expected to be similar in the East and West hemispheres, so that the difference between their respective rates is robust and allows to infer the R.A. modulation in a clean way.

The main results of the Fourier analysis above 4 EeV are presented in Table 1 and Figs. 1 and 2. The result for the cumulative bin with $E > 8$ EeV, which led to the first identification of the dipolar modulation of UHECRs [1], has now a significance of 6.8σ for the modulation in R.A. We also report the results obtained in the four energy bins [4, 8], [8, 16], [16, 32] and > 32 EeV. Note that the right-ascension modulation in the individual bin [8, 16] EeV has now reached a significance of

PoS(UHECR2024)008

E [EeV]	N	$d_\perp$ [%]	d_z [%]	d [%]	α_d [°]	δ_d [°]	$P(\geq r_1^\alpha)$
4-8	118,722	$1.0^{+0.6}_{-0.4}$	-1.3 ± 0.8	$1.7^{+0.8}_{-0.5}$	92 ± 28	-52^{+21}_{-19}	0.14
≥8	49,678	$5.8^{+0.9}_{-0.8}$	-4.5 ± 1.2	$7.4^{+1.0}_{-0.8}$	97 ± 8	-38^{+9}_{-9}	8.7×10^{-12}
8-16	36,658	$5.7^{+1.0}_{-0.9}$	-3.1 ± 1.4	$6.5^{+1.2}_{-0.9}$	93 ± 9	-29^{+11}_{-12}	1.4×10^{-8}
16-32	10,282	$5.9^{+2.0}_{-1.8}$	-7 ± 3	$9.4^{+2.6}_{-1.9}$	93 ± 16	-51^{+13}_{-13}	4.3×10^{-3}
≥32	2,738	11^{+4}_{-3}	-13 ± 5	17^{+5}_{-4}	144 ± 18	-51^{+14}_{-14}	9.8×10^{-3}

Table 1: Results for the 3D dipole reconstruction in the range of full efficiency of the SD-1500 array. For each energy bin the number of events, N, the equatorial component of the amplitude, $d_\perp$, the North-South component d_z, the amplitude d, the R.A., α_d, and declination, δ_d, of the dipole direction and the probability of getting a larger amplitude from fluctuations of an isotropic distribution $P(\geq r_1^\alpha)$ are presented.

$5.7\,\sigma$.

The dipolar amplitudes in the different bins are found to increase with energy, as is also shown in the left panel of Fig. 2, and they can be approximately described with a power-law as $d(E) = d_{10}(E/10\,\mathrm{EeV})^\beta$, where $d_{10} = 0.049 \pm 0.009$ and $\beta = 0.97 \pm 0.21$. The direction of the dipoles in all energy bins point more than 100° away from the Galactic center (GC), as shown in the right panel of the figure, indicating that the CRs are mostly extragalactic in this energy range.

Allowing also for a quadrupolar modulation to be present, one can reconstruct all the different associated components and the results obtained are shown in Table 2. One can see that the reconstructed dipole components are essentially consistent with those obtained before under the assumption of a purely dipolar modulation, and that none of the quadrupolar components has a large significance. Also, applying a multipolar analysis including multipoles up to $\ell = 20$ along the lines of ref. [10] we do not find significant amplitudes beyond that of the dipole above 8 EeV, as illustrated in Fig. 3.

The results obtained for the equatorial dipole components at lower energies, using the East-West method in the bins in which the array is not fully efficient, are reported in Table 3 and Fig. 4 for different bins down to an energy of 0.03 EeV. One can see that below 8 EeV none of the amplitudes

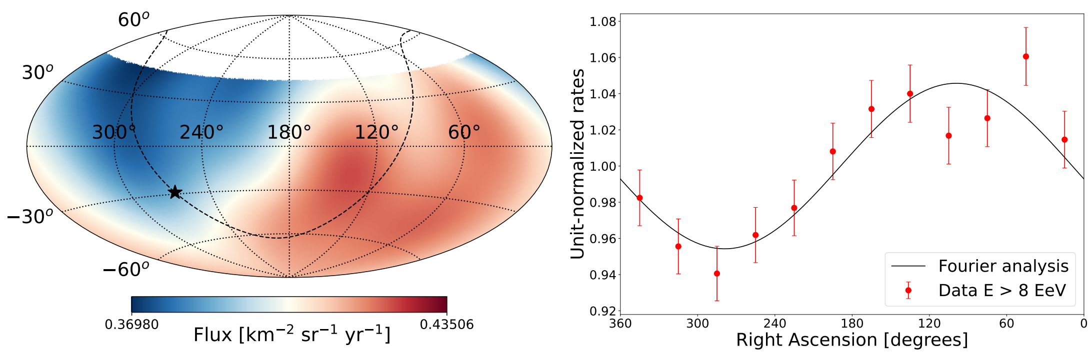

Figure 1: Left: Flux above 8 EeV in equatorial coordinates, smoothed on a 45° radius window. The Galactic Plane is represented with a dashed line and the Galactic Center is indicated with a star. Right: Distribution in R.A. of the rates of events with $E \geq 8$ EeV, normalized to a unit average. The black line shows the obtained distribution with the Fourier analysis assuming only a dipolar component.

PoS(UHECR2024)008

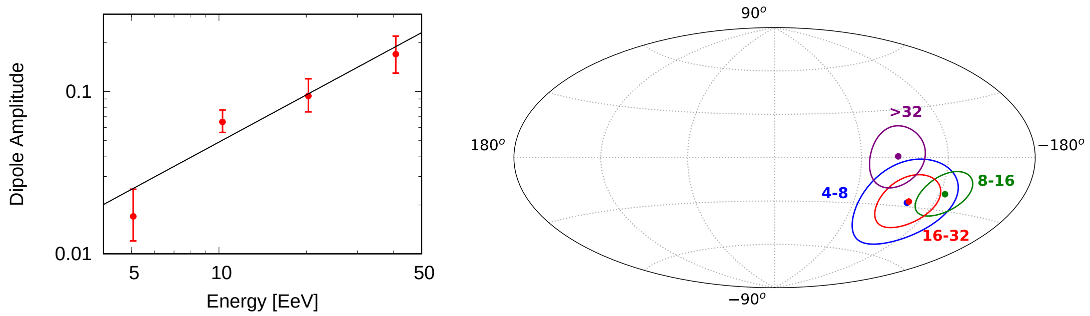

Figure 2: Left: The evolution of the dipole amplitude with energy for the four energy bins considered (4-8, 8-16, 16-32, ≥ 32) EeV. Right: Map with the directions of the 3D dipole for different energy bins, in Galactic coordinates. Shown are the contours of equal probability per unit solid angle, marginalized over the dipole amplitude, that contain the 68% CL range.

has less than 1% probability of resulting from fluctuations of an isotropic distribution, and the resulting 99% CL upper bounds on the equatorial dipole amplitudes are indicated with horizontal bars, being typically at the level of 1 to 2%. However, one remarkable finding is that below 2 EeV the right ascension phases appear to be consistently aligned with values close to that of the Galactic center ($\sim 270°$). This may be related to the presence of a surviving Galactic component with a sizable intrinsic anisotropy partly contributing in this energy range, but may eventually also be due to a different extragalactic contribution being present below few EeV and being affected by the Galactic magnetic field deflections. For comparison, we also include the results obtained at lower energies by the KASCADE-Grande and IceCube collaborations, which are consistent with a smooth extrapolation of our results.

A natural explanation for the findings at the highest energies is that the dipolar modulation reflects the anisotropy in the distribution of the nearby extragalactic cosmic-ray sources, eventually reshaped by the deflections due to the Galactic and extragalactic magnetic fields. In particular, the

	4–8 EeV	≥ 8 EeV	8–16 EeV	16–32 EeV	≥ 32 EeV
d_x	-0.003 ± 0.007	-0.002 ± 0.011	-0.002 ± 0.012	0.029 ± 0.024	-0.1 ± 0.5
d_y	0.005 ± 0.007	0.059 ± 0.011	0.048 ± 0.012	0.088 ± 0.024	0.1 ± 0.5
d_z	0.002 ± 0.019	-0.02 ± 0.03	0.02 ± 0.04	-0.15 ± 0.07	-0.23 ± 0.13
Q_{zz}	0.03 ± 0.03	0.04 ± 0.05	0.10 ± 0.06	-0.13 ± 0.13	-0.16 ± 0.25
$Q_{xx} - Q_{yy}$	0.018 ± 0.025	0.07 ± 0.04	0.03 ± 0.04	0.18 ± 0.08	0.30 ± 0.17
Q_{xy}	-0.016 ± 0.012	0.026 ± 0.019	0.041 ± 0.022	-0.05 ± 0.04	0.11 ± 0.08
Q_{xz}	-0.010 ± 0.016	0.017 ± 0.025	0.003 ± 0.029	0.10 ± 0.06	-0.10 ± 0.10
Q_{yz}	-0.019 ± 0.016	0.005 ± 0.025	-0.029 ± 0.029	0.09 ± 0.06	0.13 ± 0.10
Q	0.018 ± 0.010	0.028 ± 0.015	0.05 ± 0.02	0.10 ± 0.03	0.13 ± 0.06
$Q^{\rm UL}$	0.04	0.05	0.08	0.15	0.26

Table 2: Results obtained considering both dipolar and quadrupolar components. The dipole components, $\mathbf{d} = (d_x, d_y, d_z)$, the five independent quadrupolar components, Q_{ij}, the quadrupole amplitude, Q (such that $Q^2 = \sum Q_{ij}^2/9$), and the 99% CL upper limit, $Q^{\rm UL}$, are presented. The x-axis lies along the $\alpha = 0$ direction.

PoS(UHECR2024)008

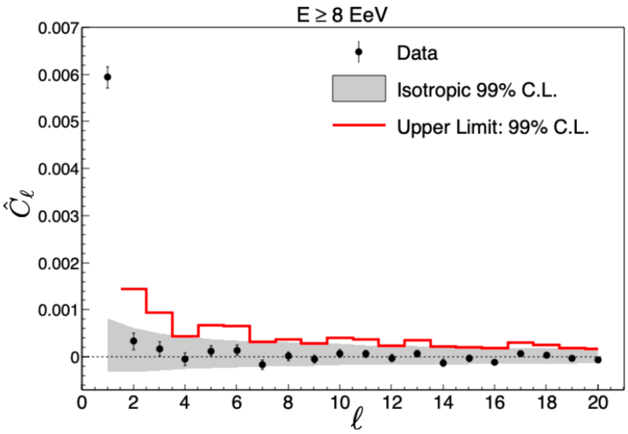

Figure 3: Angular power spectrum measurements for $E \geq 8$ EeV. The gray bands correspond to the 99% CL fluctuations that would result from an isotropic distribution. The red lines correspond to the 99% CL upper limits.

distribution of galaxies within 100 Mpc is known to be non-uniform, having a dipolar component more or less aligned with the dipole observed in the cosmic microwave background (since our peculiar velocity points approximately in the direction towards the excess of nearby galaxies). If the UHECR sources were to be distributed in a similar way as the galaxies, one should then expect to observe an anisotropy correlated to that of the distribution of galaxies, somewhat distorted by the coherent deflections that the charged CRs suffer as they enter the Galaxy and until they reach the Earth. In addition, a departure from a dipolar distribution could also be expected in association to e.g. the Supergalactic plane, along which the density of galaxies is enhanced. The fact that for increasing energies the distance from which the UHECRs can reach us gets reduced should also lead to a growth of the dipolar amplitude with energy. This is due to the fact that the very faraway sources are expected to lead to a more isotropic CR distribution and hence their contribution, which is not suppressed at low energies, would tend to dilute the total dipole.

		E [EeV]	N	$d_\perp$(%)	α_d [°]	$P(\geq r_1^\alpha)$	$d_\perp^{\rm UL}$(%)
SD750	East – West	1/32-1/16	1,811,897	$0.8^{+0.5}_{-0.3}$	110 ± 31	0.22	1.9
		1/16-1/8	1,843,507	$0.6^{+0.4}_{-0.2}$	-69 ± 32	0.23	1.5
		1/8-1/4	607,690	$0.4^{+0.7}_{-0.1}$	-44 ± 68	0.79	1.8
	Fourier	0.25-0.5	135,182	$0.5^{+0.6}_{-0.2}$	-107 ± 55	0.65	1.7
SD1500	East – West	0.25-0.5	930,942	$0.5^{+0.5}_{-0.2}$	-132 ± 47	0.51	1.7
		0.5 - 1	3,049,342	$0.4^{+0.3}_{-0.2}$	-95 ± 35	0.28	1.0
		1-2	1,639,139	$0.1^{+0.4}_{-0.1}$	-84 ± 88	0.93	1.0
	Fourier	2-4	380,491	$0.4^{+0.3}_{-0.2}$	-41 ± 38	0.36	1.2

Table 3: Results for the large scale analysis in R.A.. For each energy bin, the number of events, N, the equatorial component of the amplitude, $d_\perp$, the R.A. of the dipole direction, α_d, the probability of getting a larger amplitude from fluctuations of an isotropic distribution, $P(\geq r_1^\alpha)$, and the 99% CL upper limit, $d_\perp^{\rm UL}$, are presented.

PoS(UHECR2024)008

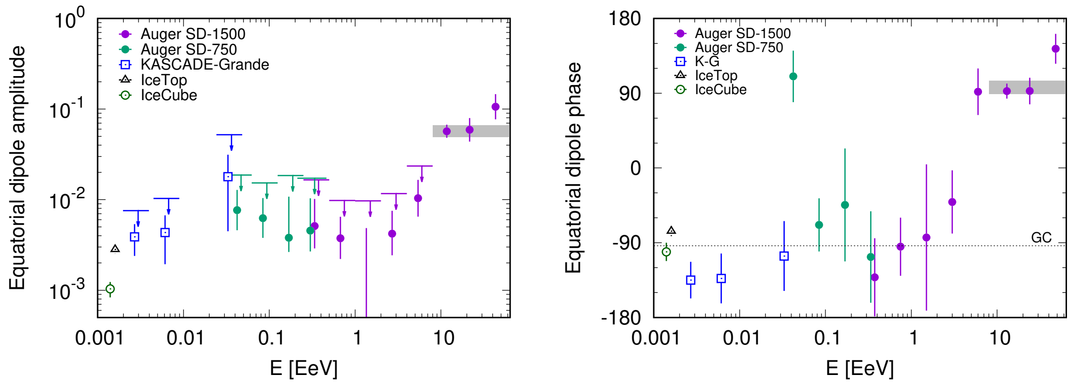

Figure 4: Equatorial dipole amplitude (left) and phase (right) for the energy bins where the dataset from the SD-1500 array (purple circles) or the SD-750 array (green circles) are used. The 99% CL upper limits for the energy bins in which the obtained amplitude has a P($\geq r_1^\alpha$)> 1% are shown. Results from the IceCube [12] and KASCADE-Grande [11] collaborations are also included for comparison.

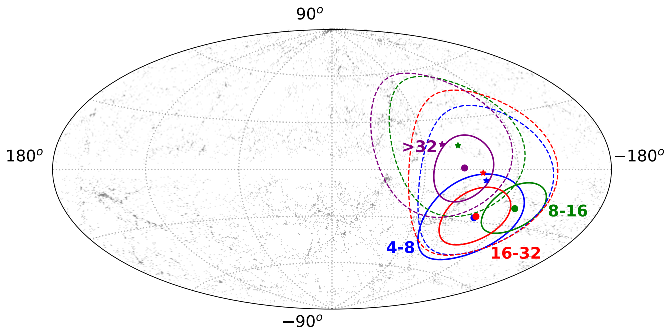

Figure 5: Map in Galactic coordinates showing the predictions for the direction of the mean dipole (star symbols) and the 68% CL contour regions (dashed lines) obtained for 10^3 realizations of the source distribution for a density of 10^{-4} Mpc^{-3} and for each energy bin above 4 EeV. This is compared to what obtained in data (continuous lines). The gray dots represent the location of the galaxies in the IR catalog within 120 Mpc.

.

As an example, we show in Fig. 5 the expected dipole direction in the different energy ranges, and in Fig. 6 the expectations for the dipolar and quadrupolar amplitudes, for scenarios in which the UHECR sources are sampled from a volume-limited catalog obtained from the 2MRS galaxies. Different source densities are considered, with a spectrum and composition following those inferred from a combined fit to the corresponding measurements [13] and considering the deflections produced by the JF12 Galactic magnetic-field model [14]. Comparing these predictions with the measurements one can see that a general agreement between their main features is obtained.

Continued observations in the coming years are expected to significantly constrain these scenarios, as well as alternative ones, helping to identify the sources of UHECRs in the near future. In particular, the upgrade of the Auger Observatory [15], which is now becoming operational, will be crucial to achieve these goals.

PoS(UHECR2024)008

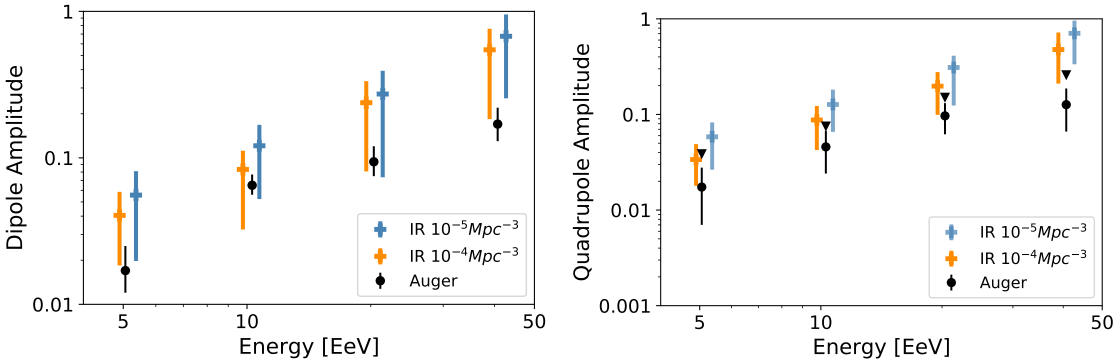

Figure 6: Left: Median and 68% CL range of the dipole amplitudes for the two source densities considered, 10^{-4} Mpc^{-3} (orange) and 10^{-5} Mpc^{-3} (blue). Right: Expected values of the average quadrupole amplitude, Q, for the same model of the high-energy population of sources. In both plots the results from data are shown (black dots) and for the average quadrupole amplitude the 99% CL upper limits are included (black triangles). The four energy ranges are (4-8, 8-16, 16-32, $\geq$ 32) EeV.

References

[1] A. Aab et al. (Pierre Auger Collaboration), Science 357 (2017) 1266

[2] A. Aab et al. (Pierre Auger Collaboration), Astrophys. J. 868 (2018) 4

[3] P. Abreu et al. (Pierre Auger Collaboration), Eur. Phys. J. C 81 (2021) 966

[4] A. Aab et al. (Pierre Auger Collaboration), Phys. Rev. D 90 (2014) 122006

[5] A. Abdul Halim et al. (Pierre Auger Collaboration), Phys. Rev. Lett. 134 (2025) 2, 021001

[6] A. Abdul Halim et al. (Pierre Auger Collaboration), Astrophys. J. 976 (2024) 48

[7] A. Aab et al. (Pierre Auger Collaboration), JINST 12 (2017) P02006

[8] A. Aab et al. (Pierre Auger Collaboration), JCAP 11 (2011) 022

[9] R. Bonino et al., Astrophys. J. 738 (2011) 67

[10] A. Aab et al. (Pierre Auger Collaboration), JCAP 06 (2017) 026

[11] W. D. Apel et al. (KASCADE-GRANDE Collaboration), Astrophys. J. 870 (2019) 91

[12] M.G. Aartsen et al. (Icecube Collaboration), Astrophys. J. 826 (2016) 220746

[13] A. Abdul Halim et al. (Pierre Auger Collaboration), JCAP 05 (2023) 024

[14] R. Jansson and G.R. Farrar, Astrophys. J. 757 (2012) 14

[15] A. Aab et al. (Pierre Auger Collaboration), (2016) arXiv:1604.03637 [astro-ph]

PoS(UHECR2024)008